scientific reports

OPEN

Synergistic effect of synthetic derivatives of 1,3,4-thiadiazole with amphotericin B in antifungal therapy

Dominika Kubera[1✉], Adrianna Sławińska-Brych[1], Agnieszka Dróźdż[2], Alina Olender[3], Agnieszka Bogut[3], Arkadiusz Matwijczuk[4], Dariusz Karcz[5], Magdalena Kimsa-Dudek[6], Joanna Magdalena Gola[7], Celina Kruszniewska-Rajs[7], Jolanta Adamska[7], Magdalena Szukała[8], Wojciech Dąbrowski[8], Andrzej Stepulak[9] & Mariusz Gagoś[1✉]

Amphotericin B (AmB) is a potent antifungal agent with minimal resistance among clinical isolates, but its use is limited by severe side effects. Reducing its toxicity through combination therapy with synergistic compounds is a promising strategy. This study investigates the antifungal potential of 1,3,4-thiadiazole derivatives, focusing on AT2 and AT10, against *Candida* species. AT2 demonstrated the highest activity, achieving complete inhibition at 128 µg/mL and notable suppression at lower concentrations. The combination of AT2 and AT10 with amphotericin B exhibited synergistic effects, leading to significant structural alterations in the fungal cell wall, including reduced β-glucan levels and increased synthesis of mannan and phosphomannan. These modifications correlated with enhanced antifungal efficacy without exacerbating cytotoxicity toward human fibroblasts and renal epithelial cells. The spectroscopic analysis suggested that the synergy arose from both cell wall disruptions and amphotericin B disaggregation. These findings highlight the potential of thiadiazole-based combination therapies for combating resistant fungal infections.

Keywords *Candida*, Antifungals, Combination therapy, Amphotericin B

Candida species belong to the group of commensal microorganisms that occur on the skin and mucous membranes of the oral cavity, gastrointestinal tract, and urogenital tract of humans. A significant reduction in immunity caused by, for example, cancer, organ transplants, immunosuppressive drug therapy, antibiotics, chemotherapy, or hemodialysis can lead to severe invasive infections[1]. In recent years, *Candida albicans* has been the primary species of *Candida* isolated from patients with invasive candidiasis. Currently, there has been an increase in infections caused by non-albicans species, which account for about 50% of all infections[1–3].

Systemic antifungal drugs are used to treat invasive candidiasis. Four classes of preparations are distinguished, differing in their mechanisms of action. The most commonly used are echinocandins (micafungin, anidulafungin, caspofungin) and azoles (fluconazole, itraconazole, voriconazole) characterized by low toxicity; however, due to the increasingly frequent occurrence of multidrug-resistant species, therapy with these drugs may often prove

[1]Department of Cell Biology, Maria Curie-Sklodowska University, Akademicka 19, 20-033 Lublin, Poland. [2]Faculty of Physics and Applied Computer Science, AGH University of Krakow, al. A. Mickiewicza 30, 30-059 Krakow, Poland. [3]Chair and Department of Medical Microbiology, Medical University of Lublin, Chodzki 1 Street, 20-093 Lublin, Poland. [4]Department of Biophysics, Faculty of Environmental Biology, University of Life Sciences in Lublin, Akademicka 13, 20-950 Lublin, Poland. [5]Department of Chemical Technology and Environmental Analytics, Cracow University of Technology, 31-155 Krakow, Poland. [6]Department of Nutrigenomics, and Bromatology, Faculty of Pharmaceutical Sciences in Sosnowiec, Medical University of Silesia, 40-055 Katowice, Poland. [7]Department of Molecular Biology, Faculty of Pharmaceutical Sciences in Sosnowiec, Medical University of Silesia, 40-055 Katowice, Poland. [8]First Department of Anesthesiology and Intensive Therapy, Medical University of Lublin, Jaczewskiego Street 8, 20-090 Lublin, Poland. [9]Department of Biochemistry and Molecular Biology, Medical University of Lublin, Chodzki 1 Street, 20-093 Lublin, Poland. ✉email: dominika.kubera@mail.umcs.pl; mariusz.gagos@mail.umcs.pl

ineffective[4]. The strongest and oldest antifungal antibiotic used in the treatment of invasive fungal infections is amphotericin B. This agent belongs to the group of polyene antibiotics and is characterized by a broad spectrum of activity and strong fungicidal action. Moreover, most *Candida* species maintain sensitivity to polyenes. Due to its toxicity at higher concentrations, amphotericin B is used only in severe systemic infections[5,6].

Microbial resistance to antibiotics poses a significant problem worldwide. Despite ongoing efforts to develop new therapies, the resistance continues to rise, leading to a substantial reduction in the effectiveness of available antimicrobial agents. Therefore, it is extremely important to develop new alternative antimicrobial agents with different mechanisms of action and therapies that can increase the effectiveness of currently used antibiotics[7,8].
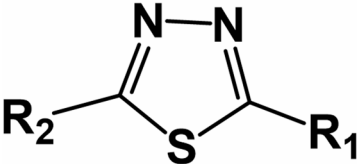
Drug interactions in combination therapy can be divided into two types: synergistic and antagonistic. Synergistic interactions occur when the combined effect of both substances is more effective than the action of a single agent. Antagonism occurs when one of the substances used decreases the effectiveness of any of the agents used alone. To determine the type of interaction, the checkerboard test is often used, where a two-dimensional array of serial concentrations of the compounds studied serves as the basis for calculating the fractional inhibitory concentration index (FICI)[9].

In our studies, we focused on searching for substances that exhibit synergy with amphotericin B (AmB). A group of synthetic derivatives of 1,3,4-thiadiazole, characterized by antimicrobial activity and synergy with AmB, was subjected to testing, as reported in our previous publications[10–13]. Based on our previous results and extensive preliminary studies, we selected another group of compounds with a similar structure, guided by their potential biological activity. The aim was to conduct a more detailed investigation of their fungicidal activity and possible interactions with antibiotics. The experiments involved two reference strains of *Candida* fungi with different sensitivities to AmB. Substances demonstrating synergistic activity with the antibiotic underwent further testing to evaluate their toxicity. The molecular mechanisms of the antifungal action of the antibiotics and their combinations against *C. albicans* cells were analyzed using ATR-FTIR (attenuated total reflection Fourier transform infrared spectroscopy) and electron absorption and fluorescence methods. Additionally, the toxicity of selected combinations against human skin fibroblasts (NHDF) and renal epithelial cells (RPTEC) was investigated.

Results

Study of antifungal activity

The structures of the 1,3,4-thiadiazole derivatives tested are presented in Fig. 1. The results illustrating the activity of individual substances against *Candida* strains are presented in Fig. 2. Among the 10 selected substances, AT2 exhibited the greatest inhibition of *Candida* growth.

The values for the minimum inhibitory concentration for 100% fungal growth inhibition (MIC_{100}) obtained after 48 h for both reference strains were 128 µg/mL. At a concentration of 16 µg/mL, approximately 40% growth inhibition, compared to the control (medium with the yeast only), was observed. The substance designated as AT1 inhibited the growth of the fungi by approximately 90–100%, depending on the strain after 24 h of

Compound	R_1	R_2
AT1	–NH_2	–2,4–dihydroxyphenyl
AT2	–NH_2	–2–hydroxyphenyl
AT3	–NH–CH_3	–2,4–dihydroxyphenyl
AT4	–NH_2	–2,4–dinitrophenyl
AT5	–NH_2	–4–nitrophenyl
AT6	–NH_2	–phenyl
AT7	–NH_2	–4–methoxyphenyl
AT8	–NH_2	–SH
AT9	–NH_2	–S–CH_2–CH_3
AT10	–NH_2	–*t*–butyl

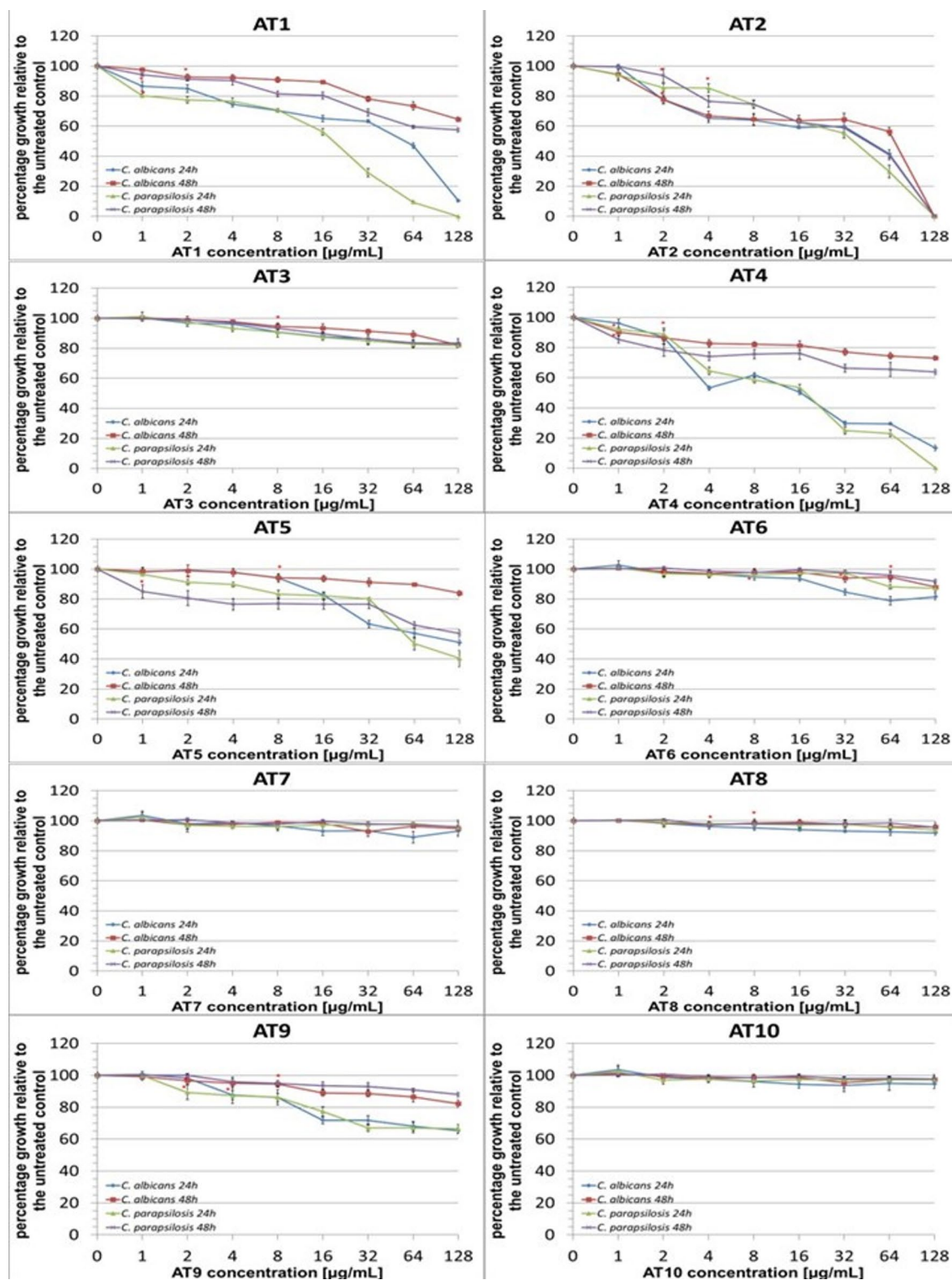**Fig. 1**. Structures of 1,3,4-thiadiazole derivatives tested.

Fig. 2. Percentage growth of *C. albicans* NCPF 3153 and *C. parapsilosis* ATCC 22,019, measured as OD600, induced by selected derivatives of 1,3,4-thiadiazoles in relation to the control. Fungi were cultured in 96-well plates according to the procedure for determining MIC. Optical density was measured spectrophotometrically at a wavelength of 600 nm after 24 and 48 h of incubation at 35 °C. The plotted values are expressed as the mean ± SD from three measurements performed in three repetitions (*n* = 9). The percentage growth of treated samples, compared to the control, was calculated using the following equation: (OD600 of the treated sample) / (OD600 of the untreated sample) x 100. *The lowest concentration at which a statistically significant decrease in OD, compared to the control, was recorded (ANOVA analysis and Tukey's post-hoc test).

incubation at the highest tested concentration. After an additional day of incubation, a sharp increase to about 57–64% of the control was noted. AT6 demonstrated weaker fungistatic activity, compared to the aforementioned analogs. Derivatives AT4 and AT5 showed higher inhibitory activity than that of AT6, resulting in a complete lack of growth of *C. parapsilosis* after 24 h at a concentration of 126 µg/mL. The activity of thiadiazole AT8 was weaker than in the case of AT6, while AT9 exhibited greater activity after 24 h, inhibiting the growth of *Candida* by approximately 35%.

Interactions of thiadiazoles with antibiotics

To investigate the interactions of selected thiadiazoles with antibiotics, the broth microdilution checkerboard method was used. The experiment was conducted on five reference strains: *Candida albicans* NCPF 3153, *Candida parapsilosis* ATCC 22,019, *Candida krusei* ATCC 1424, *Candida glabrata* ATCC 15,126 and *Candida tropicalis* ATCC 13,803. To obtain the most reliable results, readings were taken after 24 and 48 h of incubation. Some of the compounds used separately at the concentrations selected for the experiment showed no inhibitory activity. Consequently, the MIC value of AT10 was not determined. To calculate the FICI value, we used a twofold higher concentration of AT10 (256 µg/mL) to illustrate the type of interaction. Among the 10 derivatives of thiadiazoles, only two showed interactions with amphotericin B (Table 1). None of the tested compounds demonstrated interactions with fluconazole. No antagonistic interactions ($\Sigma FIC \geq 2$) were observed in any of the tested strains at any concentration. Compounds AT2 and AT10 exhibited synergistic effects ($\Sigma FIC \leq 0.5$) with AmB at a concentration of 32 µg/mL against *C. albicans* and at a concentration of 64 µg/mL for *C. parapsilosis*. In the case of *Candida krusei*, AT2 exhibited additivity, while AT10 displayed synergy. For *Candida glabrata*, a synergistic effect was observed only with AT2; the AT10-AmB combination showed no interaction. Regarding *Candida tropicalis*, no interaction was found between AT2 and AmB, whereas the AT10-AmB combination exhibited additivity. Only these two compounds (AT2 and AT10) were selected for further studies, as they demonstrated a synergistic effect with AmB.

Cytotoxicity of selected thiadiazoles (AT2 and AT10), AmB, and their combinations against normal NHDF and RPTEC cells

First, the cytotoxicity of AmB applied separately against normal human dermal fibroblasts (NHDF) was estimated by the NR test after 48 h. In this method, living cells with intact lysosomal and cell membranes have the ability to uptake and concentrate neutral red in lysosomes. As shown in Fig. 3A, AmB caused a marked reduction in the vitality of normal cells from the concentration of 10 µg/mL, but the lower doses did not damage the cell membrane. The toxicity of AT2 used alone and in combination with AmB was then assessed in the same culture conditions. It was found that AT2 in the concentration range of 4–64 µg/mL had no toxic effect against the NHDF cells. However, a rapid decrease in NR accumulation (suggesting cell death induction) was observed at the higher doses. When the cultures were treated with the doses of 128 µg and 264 µg, cell survival dropped to almost 50% and 15%, respectively (Fig. 3B). Also, the 48-hour co-incubation of the NHDF cells with AmB (0.125 and 0.25 µg/mL) and AT2 (32 and 64 µg/mL) did not impair their lysosomal activity (Fig. 3C). Interestingly, after the simultaneous incubation of the cells with AT2 at a concentration of 64 µg/mL, a significant increase in cell survival was even observed. The obtained results clearly indicate that AT2 does not potentiate the toxicity of AmB against human skin fibroblasts. The same assay was also used to estimate the number of live cells after the treatment with AT10 and its combination with AmB. The NR measurements demonstrated (Fig. 4A) that AT10 used at concentrations up to 128 µg/mL had no destructive impact on the normal cells. An apparent decrease in the cell viability (by about 20%) was observed only after applying the highest (256 µg/mL) concentration of this compound. Furthermore, the NHDF cultures treated with a mixture of AT10 and AmB (at both concentrations tested) showed comparable levels of cellular vitality to that of the untreated cells (Fig. 4B).

The nephrotoxic effect of thiadiazoles may be one of the factors limiting their potential use in the treatment of systemic fungal infections in both mono- and combined therapy. Therefore, we conducted additional experiments on human renal proximal tubule cells (RPTEC) to exclude the potential toxicity of these compounds and their mixture with AmB. Based on the obtained results, it can be concluded that AmB in doses up to 1 µg/mL did not have a lethal effect on RPTEC cultures (Fig. 5A). Moreover, AT10 applied in a wide range of concentrations from 0.5 to 64 µg/mL did not exhibit toxic activity against renal cells. At concentrations ranging from 0.5 µg/mL to 16 µg/mL, the viability of RPTEC cells remained at a level similar to or higher than the control, indicating a lack of significant cytotoxicity (Fig. 5B). For instance, at a concentration of 8 µg/mL, the cell viability was 102.89%, compared to the control. Even at the higher concentrations of, such as 32 and 64 µg/mL, the cytotoxicity of AT10 was minimal, with cell viability at 100.71% and 97.45%, respectively. Additionally, in the study of the action of AT10 in combination with amphotericin B, it was observed that the combination of these two substances did not lead to a significant reduction in RPTEC cell viability (Fig. 5C). In the combinations of AT10 at the concentrations of 4, 8, and 16 µg/mL with amphotericin B at the concentrations ranging from 0.125 to 1 µg/mL, cell viability remained close to the control level. The highest viability, at 110.15%, was observed in the combination of 16 µg/mL AT10 and 1 µg/mL amphotericin B, suggesting that AT10 not only does not increase the cytotoxicity of amphotericin B but may also have a protective effect on RPTEC cells in some cases. Our results may therefore provide evidence supporting the potential of the combination of AT2 or AT10 with AmB as a promising tool for use in antifungal therapy of skin or other organs.

Selectivity index of the tested compounds

The SI was calculated to determine the usefulness of the tested compounds (AT2 and AT10) in the treatment of mycosis in humans. The SI value higher than 1 indicates that the drug efficacy against fungal cells is greater than its toxicity against host cells. Table 2 indicates the SI values of the tested thiadiazole derivatives (AT2 and AT10),

Microorganism	Agent	MIC (µg/mL)		FIC	FICI	Type of interaction
		Alone	Combination			
24-h incubation						
Candida albicans NCPF 3153	AT2	128	32	0.25	0.5	Synergy
	AmB	0.25	0.0625	0.25		
	AT10	>128	32	0.125	0.375	Synergy
	AmB	0.25	0.0625	0.25		
Candida parapsilosis ATCC 22019	AT2	128	64	0.5	0.75	Additivity
	AmB	0.5	0.125	0.25		
	AT10	>128	64	0.25	0.5	Synergy
	AmB	0.5	0.125	0.25		
Candida krusei ATCC 1424	AT2	64	32	0.5	0.75	Additivity
	AmB	0.5	0.125	0.25		
	AT10	>128	64	0.25	0.375	Synergy
	AmB	0.5	0.0625	0.125		
Candida glabrata ATCC 15126	AT2	64	16	0.25	0.5	Synergy
	AmB	1	0.25	0.25		
	AT10	>128	64	0.25	1.25	No interaction
	AmB	1	1	1		
Candida tropicalis ATCC 13803	AT2	128	64	0.5	1.5	No interaction
	AmB	0.25	0.25	1		
	AT10	>128	64	0.25	0.75	Additivity
	AmB	0.25	0.125	0.5		
48-h incubation						
Candida albicans NCPF 3153	AT2	128	32	0.25	0.5	Synergy
	AmB	0.5	0.125	0.25		
	AT10	>128	32	1.25	0.375	Synergy
	AmB	0.5	0.125	0.25		
Candida parapsilosis ATCC 22019	AT2	128	64	0.5	0.75	Additivity
	AmB	1	0.25	0.25		
	AT10	>128	64	0.25	0.5	Synergy
	AmB	1	0.25	0.25		
Candida krusei ATCC 1424	AT2	64	32	0.5	0.625	Additivity
	AmB	1	0.125	0.125		
	AT10	>128	64	0.25	0.375	Synergy
	AmB	1	0.125	0.125		
Candida glabrata ATCC 15126	AT2	64	32	0.5	0.75	Additivity
	AmB	1	0.25	0.25		
	AT10	>128	64	0.25	1.25	No interaction
	AmB	1	1	1		
Candida tropicalis ATCC 13803	AT2	128	64	0.5	1.5	No interaction
	AmB	0.5	0.5	1		
	AT10	>128	64	0.25	0.75	Additivity
	AmB	0.5	0.25	0.5		

Table 1. Interactions of thiadiazoles AT2 and AT10 with amphotericin B (AmB) in combating reference strains in vitro after 24 and 48 h of incubation.

which were calculated using the MIC of the drug alone and in the mixture with AmB. As presented in Table 2, both AT2 and AT10 alone and in combinations may have potential therapeutic benefits (SI > 1).

ATR-FTIR analysis of biomolecular mechanisms of activity in the combinations of 1,3,4-thiadiazole derivatives with amb in *C. albicans*

The average IR spectra and their inverted second derivatives for *C. albicans* cells subjected to the action of AT2 (32 µg/mL), AmB (0.06 µg/mL), and their mixture are presented in Fig. 6, while the average spectra for cells exposed to AT10 (32 µg/mL), AmB (0.06 µg/mL), and their combination are shown in Fig. 8. The concentrations of thiadiazoles and AmB were chosen so that the amount of cultivated inoculum was sufficient for FTIR measurements with simultaneous observation of fungal growth inhibition. Absorption bands were identified based on the inverted second derivatives (Table 3). Differences in the intensity of the bands identified
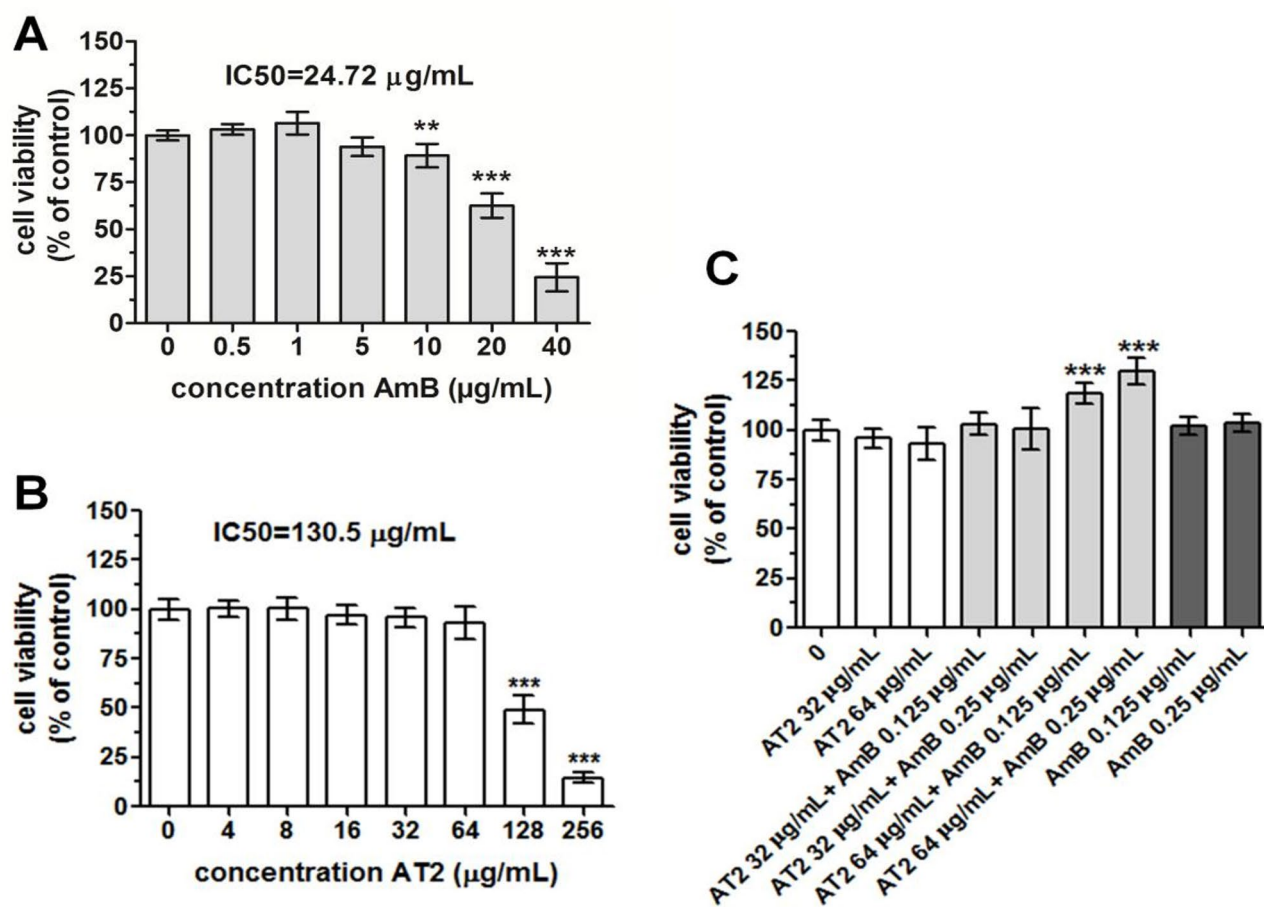
Fig. 3. Cytotoxic effect of AmB, AT2, and their combination against normal NHDF cells. The cells were incubated with AmB (**A**) and AT2 alone (**B**) or with the mixture of AmB + AT2 (**C**) for 48 h, and the cell viability was determined by the NR assay. Results were expressed as % viability of cells, compared to the vehicle (DMSO) control. Data are shown as means S.D. of three independent experiments and were analyzed by one-way ANOVA, followed by Dunnett's multiple comparison test ($p < 0.001$*** vs. Control).

for *C. albicans* in the groups exposed to AT2, AT10, their mixtures with AmB, and AmB alone were analyzed based on the peak areas calculated for the inverted second derivatives of the IR spectra in relation to the control group. The statistical significance of the observed changes was assessed using the Mann-Whitney U test at a significance level of 5%. Additionally, statistical trends were analyzed at a significance level of 10%. The results of the statistical analysis for selected bands are presented in Figs. 7 and 9.
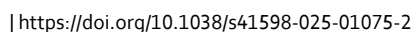
AT2

As shown in Fig. 7, the intensity of the bands at 2958 cm^{-1} and 2918 cm^{-1} associated with the asymmetric stretching vibrations of CH$_3$ and CH$_2$ groups originating from lipids and polysaccharides was statistically significantly lower for *C. albicans* treated with AmB, compared to the control group. For the bands at 2958 cm^{-1} and 1466–1372 cm^{-1}, a statistically significant increase was observed in the group treated with AT2 + AmB, compared to the control.

The area under the band at 1655 cm^{-1}, corresponding to amide I, was statistically significantly greater for *C. albicans* treated with AT2 + AmB and AT2 alone, compared to the control, with the increase in the mixture greater than that for the thiadiazole alone. A similar relationship was observed for the band at 1543 cm^{-1}, corresponding to amide II, where no increase in intensity was noted for AT2 alone.

The intensity levels of the bands corresponding to β-1,3-glucans (1152 cm^{-1}) and β-1,6-glucans (991 cm^{-1}) showed a statistically significant decrease for *C. albicans* exposed to AT2 + AmB, compared to the control. The intensity of the absorption band at 888 cm^{-1}, related to the total content of glucans and mannans, was significantly elevated in cells treated with AT2, compared to the control, while the application of AT2 + AmB resulted in a slight decrease in intensity.

The intensity of the absorption band at 961 cm^{-1} assigned to mannans was increased in *C. albicans* exposed to AT2 + AmB, compared to the control.

A slight increase in the bands originating from phosphomannans, namely 1232 cm^{-1} from the stretching vibrations of P = O bonds and 1200 cm^{-1} assigned to the asymmetric stretching vibrations of PO$_2$, was observed in the group treated with AT2.

Fig. 4. Cytotoxic effect of AmB, AT10, and their combination with AmB against normal NHDF cells. The cells were incubated with either AT10 alone (**A**) or with the mixture of AmB + AT10 (**B**) for 48 h, and the cell viability was determined by the NR assay. Results were expressed as % viability of cells, compared to the vehicle (DMSO) control. Data are shown as means S.D. of three independent experiments and were analyzed by one-way ANOVA, followed by Dunnett's multiple comparison test ($p < 0.001$*** vs. Control).

The areas under the peaks corresponding to the content of glycogen and mannans (1045 cm^{-1}) and glycogen and phosphomannans (1078 cm^{-1}) are statistically significantly higher for cells treated with the mixture of AT2 + AmB, compared to the control. This effect was not observed in the antibiotic alone-treated group. Additionally, a statistically significant decrease in the intensity of the band at 1045 cm^{-1} and the glycogen band at 1021 cm^{-1} was observed in the group treated with AT2 alone, compared to the control.

AT10
Biochemical changes, compared to the control, were also detected in *C. albicans* exposed to AmB (0.03 µg/mL) (Fig. 8), AT10, and the combination of AT10 + AmB, as shown in Fig. 9. The intensity of the bands associated with the asymmetric stretching vibrations of the CH$_2$ groups derived from lipids and polysaccharides (2918 cm^{-1}) significantly decreased when the *Candida* cells were incubated in the presence of AT10 alone. An increase in the intensity of the bands at 2958 cm^{-1} and 1466 – 1372 cm^{-1} was observed in the group treated with the combination of AT10 + AmB, compared to the control.

The areas of the peaks corresponding to amide I (1655 cm^{-1}) and amide II (1543 cm^{-1}) were statistically significantly higher for cells incubated in the presence of AT10 + AmB and AmB alone, with a greater increase observed for the mixture, compared to AmB alone.

The intensity of the bands corresponding to β-1,3-glucans (1152 cm^{-1}) and β-1,6-glucans (991 cm^{-1}) showed a statistically significant decrease for *C. albicans* exposed to AT2 + AmB, compared to the control. The intensity of the band at 991 cm^{-1} also decreased in the group treated with the antibiotic alone. The intensity of the absorption band at 888 cm^{-1}, associated with the content of glucans and mannans, was significantly increased in the AT2-treated cells, compared to the control, while the application of AT + AmB resulted in a slight decrease in the intensity of this band.

The intensity of the absorption band at 961 cm^{-1}, attributed to mannans, was increased in *C. albicans* exposed to AT10 + AmB and AmB alone, with a more significant increase in the combination of the thiazole with the antibiotic. Significant increases were observed only in the AmB-treated group for the areas of the peaks at 1232 cm^{-1}, originating from the stretching vibrations of the P = O bonds, and 1200 cm^{-1}, attributed to the asymmetric stretching vibrations of the PO$_2$ groups.

The intensity of the bands corresponding to the content of glycogen and phosphomannans (1078 cm^{-1}) and glycogen and mannans (1045 cm^{-1}) was statistically significantly higher in the group of cells treated with the mixture of AT10 + AmB, compared to the control. A significant increase in the intensity of the band at 1045 cm^{-1} was also observed in the group treated with the thiazole alone. Opposite results were obtained for the glycogen
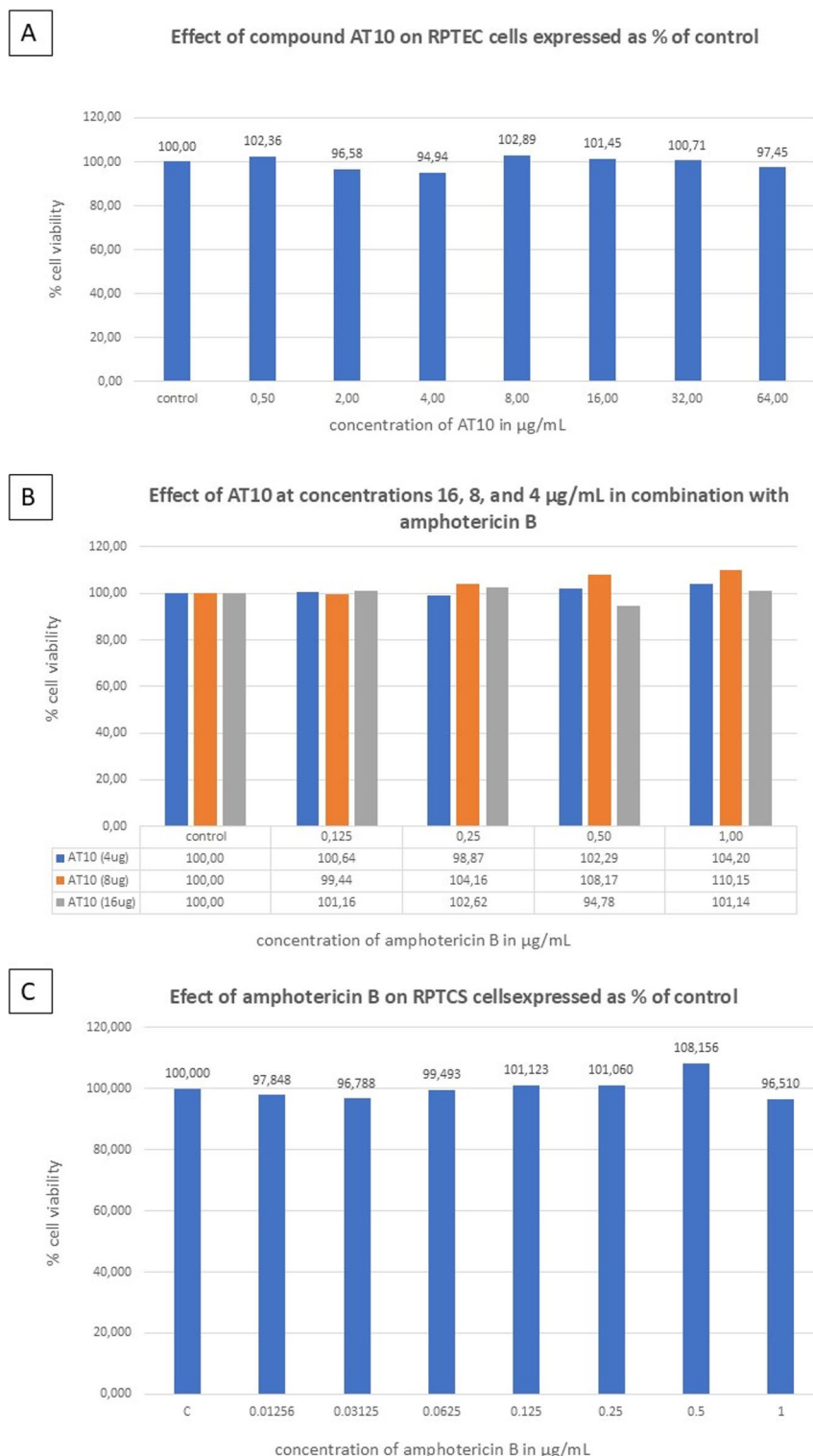
Fig. 5. Evaluation of the cytotoxicity of AT10 against RPTEC cells and its effect in combination with amphotericin B after 48 h. Effect of various concentrations of AmB (**A**) and AT10 (**B**) on RPTEC cell viability expressed as a percentage of the control. Effect of AT10 at concentrations of 4, 8, and 16 µg/mL in combination with amphotericin B on RPTEC cell viability (**C**).

Drug	IC50 NHDF (µg/mL)	Strain	Drug concentration (µg/mL)	Selectivity index (µg/mL)
AT2	130.5 ± 3.0	C. albicans	128*	1.02
			32–64**	4.08–2.04
		C. parapsilosis	128*	1.02
			64**	2.04
AT10	477.2 ± 5.0	C. albicans	256*	1.86
			32–64**	14.91–7.46
		C. parapsilosis	256*	1.86
			64**	7.45

Table 2. IC50 and SI values of the tested thiadiazoles (AT2 and AT10). *MIC of thiadiazole derivatives alone. **Range of MIC values of thiadiazole derivatives in the combination with AmB, which exhibited a synergistic effect with the antibiotic.

band (1021 cm⁻¹), for which a statistically significant decrease in intensity was observed in the group treated with AmB alone and in combination with AT10, compared to the control.

Spectroscopic analysis of synergistic interactions between selected molecules

In the subsequent stage of the study, synergistic interactions between the selected compounds from the group of *1,3,4*-thiadiazoles and amphotericin B were analyzed by spectroscopic measurements of electronic absorption and emission. First, UV-Vis spectra and the corresponding fluorescence emission spectra were recorded for all the compounds in two selected solvents with significantly different polarities, namely ethanol (EtOH) and DMSO. The detailed results are shown in Table 4. The compounds were deliberately selected to underscore potential differences between synergistic compounds, such as **AT2** and **AT10**, and those not showing such characteristics. In turn, the respective solvents were chosen to highlight differences in terms of polarity as well as other properties, e.g.: proticity (ethanol) and aproticity (DMSO). Additionally, as follows from literature, DMSO is commonly used in biological studies on various compounds, and it is also a highly solvating solvent. The reason for this particular selection of solvents stemmed from the intention to demonstrate, already at the spectral level, the relevant differences between compounds capable of synergistic interactions and those that did not reveal such potential in the conducted studies.

Examples of electronic absorption and fluorescence emission spectra registered with the adequate excitation at the maximum of the absorption band are presented in Figs. 10 and 11. Figure 10 shows the absorption spectra obtained for compound **AT2**, which displayed synergistic properties in the biological studies, while Fig. 11 shows examples of spectra registered for a compound not synergizing with AmB. As can be observed in Panels A of Figs. 10 and 11, clear wide electronic absorption bands were registered for the selected compounds. According to literature, they can be associated with π→π* electronic transitions. The positions of these bands tend to be similar in most compounds. Notably, however, this is noticeably different in some of the derivatives, which reflects structural differences between the respective chromophoric systems of the molecules. Panels B in Figs. 10 and 11 present fluorescence emission spectra corresponding to the absorption spectra discussed above. As shown in Panel B of Fig. 10, the obtained emissions differ in terms of the location of the band maxima and the intensity of fluorescence. Figure 11B presents a similar effect and the effect of dual fluorescence, well-known and described in our previous studies and by other authors, related to the phenomenon of excited state proton transfer ESIPT[15] occurring in derivatives where the groups of proton donors and acceptors are located in close vicinity to each other.

The spectra registered for the other compounds are fairly similar, with only certain noticeable differences in terms of the locations of respective absorption or emission maxima. It should be underlined, however, that such differences are primarily due to the structure (specifically length) of the chromophore systems present in the molecules selected for the study, which is certainly relevant in the context of the capacity of particular molecules for synergistic interaction or a lack thereof.

In order to find a spectroscopic explanation for the interactions observed between the selected thiadiazoles and the antibiotic, we decided to analyze the possibility of correlating Stokes shift values with the biological activity of the compounds. However, the detailed analysis of spectral shifts observed in these compounds in the two solvents used revealed no regularities that could help in choosing those with viable potential for synergistic interaction with AmB. As can be observed, the Stokes shifts registered for e.g. AT2 and AT4 are fairly similar; however, the former shows considerable synergistic capacity and the latter does not. Similar observations were made for the other compounds. Although the Stokes shift values varied from nearly similar to very different, no relevant regularities could be observed, even when accounting for molecular sizes and the polarity of the medium.

However, the results shown in Table 4 and especially in Figs. 10 and 11 do point to a certain noticeable detail, specifically a diametric change in the intensity of fluorescence emission bands. This is particularly significant in the case of the AmB molecule, as it is one of the few showing strong emission associated with aggregated forms of the compound and very weak emission associated with the monomeric forms of the molecule. Given the structure of the molecule, the results of fluorescence measurements, and our previous studies, a significant impact of aggregational interactions on the properties of the compounds, particularly their capacity for synergizing with AmB, can be hypothesized.
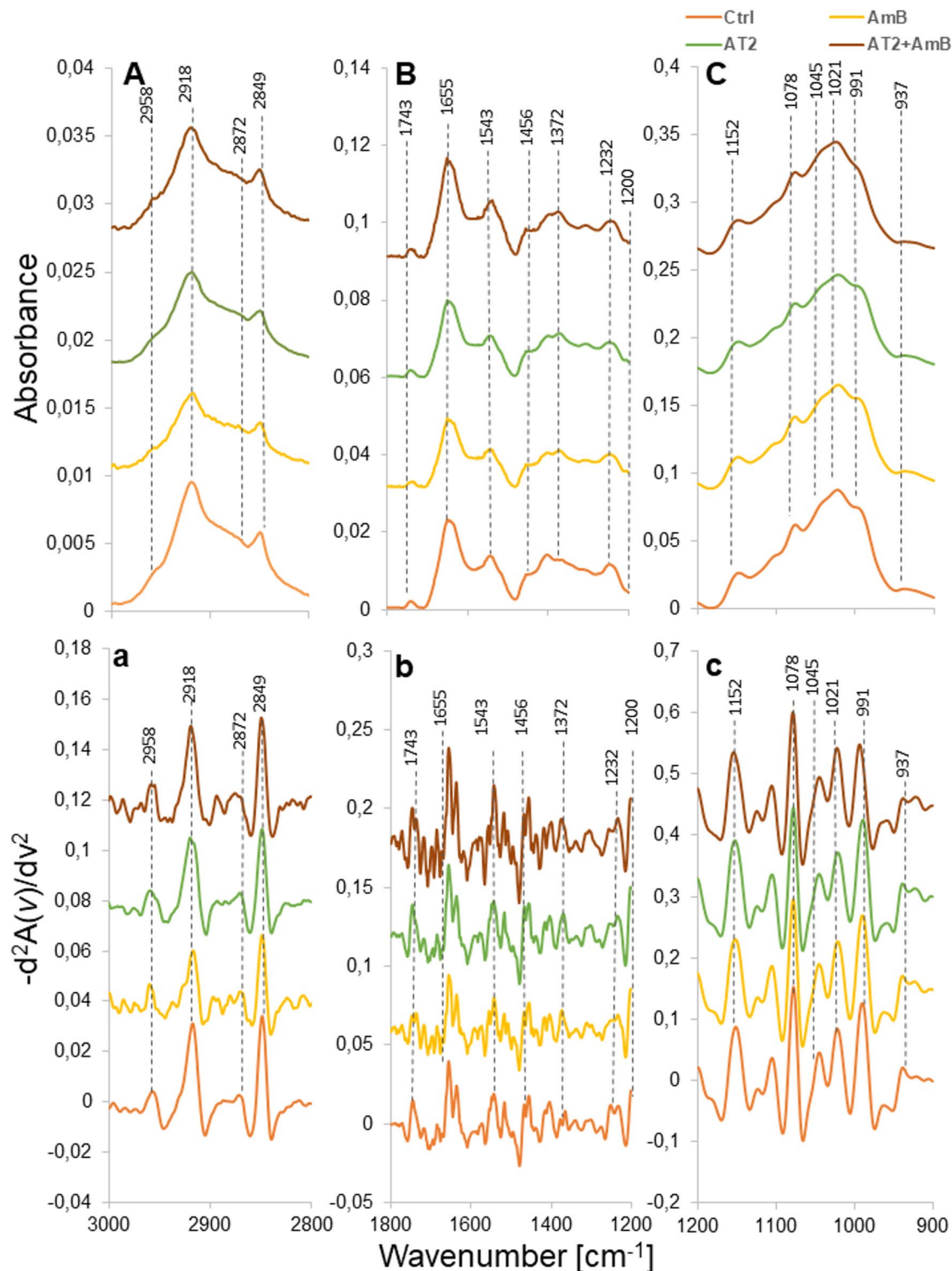
Fig. 6. Average IR spectra for *C. albicans* NCPF 3153 in the control, AmB (0.06 µg/mL), AT2 (32 µg/mL), and the combination of AT2 (32 µg/mL) and AmB (0.06 µg/mL) in the wavenumber ranges: (**A**) 3000–2800 cm⁻¹; (**B**) 1800–1200 cm⁻¹; (**C**) 1200–900 cm⁻¹; (**a**–**c**) negative second derivatives for spectra (**A**–**C**).

With a view to verifying the above hypothesis, in the subsequent step of the study we decided to measure the behavior of example absorption and fluorescence emission spectra in mixed systems, both those showing synergistic capacity and those that did not exhibit synergy. To this end, the **AT2** and **AT4** molecules were selected for further examination, and measurements were taken in mixed systems composed of the thiadiazole + AmB in DMSO. Panels A-D in Fig. 12 present the absorption and fluorescence emission spectra obtained for AT2 (Panels

Band [cm^{-1}]	Origin	Characteristic
2958	CH$_3$ str. asym.	Lipid and polysaccharide level
2918	CH$_2$ str. asym.	
2872	CH$_3$ str. sym.	
2849	CH$_2$ str. sym.	
1655	C=O str., NH bend. (Amide I)	Protein and chitin level
1543	NH bend., C–N str. (Amide II)	Protein and chitin level
1466	CH$_2$, CH$_3$ def.	Lipid, protein, and polysaccharide level
1372		
1251	NH def. (Amide III)	Protein and chitin level
1232	P=O str.	Phosphomannan level
1200	PO$_2$ str. asym.	Phosphomannan level
1152	C–O–C str.	β(1→3) glucan level
1105	CO str., CC str., C–O–C str.	Glycogen and β(1→3) glucan level
1078	PO$_2$ str. sym., CO str., CC str., C–O–H def.	Glycogen and phosphomannan level
1045	CO str., OH str. coupled with bend.	Glycogen and mannan level
1021	CO str.	Glycogen level
991	CC, C=O def.	β(1→6) glucan level
961	CC, C=O def.	Mannan level
937	CC, C=O def.	Glucan and mannan level
888		

Table 3. Identification of ATR-FTIR bands in *C. albicans* spectra. *str.* stretching, *asym.* asymmetric, *sym.* symmetric, *def.* deformation, *bend.* bending vibrations[14].

A and B) and AT4 (respectively, Panels C and D). The spectra were recorded in systems with a constant level of AmB, to which doses of compound AT2 or AT4 were gradually titrated. As can be seen in Fig. 12A, as the content of AT2 gradually increased, we mainly observed an increase in absorbance associated with the location of the band reflecting the π→π* electronic transition in the thiadiazole molecule[16], while the AmB spectrum remained practically constant. It is also noteworthy that the thiadiazole absorption band almost entirely overlaps with the region of the AmB spectrum associated with the aggregated *card pack* forms of AmB, as indicated by available literature data. Next, in the emission spectrum for AT2 presented in Fig. 12B, strong fluorescence corresponding mainly to the already presented AT2 emission spectra were observed. The spectra were fairly structured, which was related to the shape of the AmB emission spectrum, as described in literature. The obtained spectra had to be measured at lower settings due to the high quantum efficiency of AT2, compared to AmB; hence, the spectrum originating from the aggregated forms of AmB was virtually invisible due to its low intensity.

In turn, Panels C and D in Fig. 12 show analogous results obtained for the compound that showed no synergistic properties in our biological studies, i.e. AT4. The graphs indicate considerable differences from the results obtained for AT2. With the addition of AT4, the entire AmB spectrum showed a very clear increase. We observed an increase in terms of the absorption level for AmB within the range associated with its monomeric forms, with the relevant maximum at 418 nm, as shown by literature data. However, we also very clear increase in absorbance associated with the aggregated *card pack* forms of the compound, with the maximum at approx. 350 nm, was observed. A significantly increased level of absorption in the longwave range of the spectrum, with the maximum at approx. 450 nm should be noted as well. The area is typically associated with *head to tail* aggregation but can also be related to scattering among increasingly larger aggregate structures, which tends to increase absorption spectra on the longwave side. Notably, the aggregated forms were visible even in such medium as DMSO. The analysis of Panel D in Fig. 12 revealed that the results obtained with fluorescence spectroscopy, which is not a method commonly used for tracking aggregation concentrations due to fluorescence concentration quenching, also provided very interesting insights. With the increasing concentration of thiadiazole molecules, a significant decrease in fluorescence emission was observed. The emission was reduced due to the very low quantum efficiency of AmB aggregates, which constituted fairly reliable and relatively easily obtained evidence to corroborate the above hypothesis on the interaction between the molecules of the selected 1,3,4-thiadiazoles and AmB.

More interesting results providing further confirmation of the above hypotheses were provided by the fluorescence anisotropy measurements. Figure 13 presents the anisotropy values measured for the AmB molecule itself and the two selected compounds mentioned above. As follows from the data, the values of anisotropy for AmB and AT4, i.e. the non-synergistic compound, were relatively high at approximately 0.12. This confirms the significant contribution of effects related to molecular aggregation in the analyzed systems. Meanwhile, already after the addition of the first dose of AT2 into the DMSO system, the anisotropy value declined sharply to approx. 0.04, confirming significant monomerization.
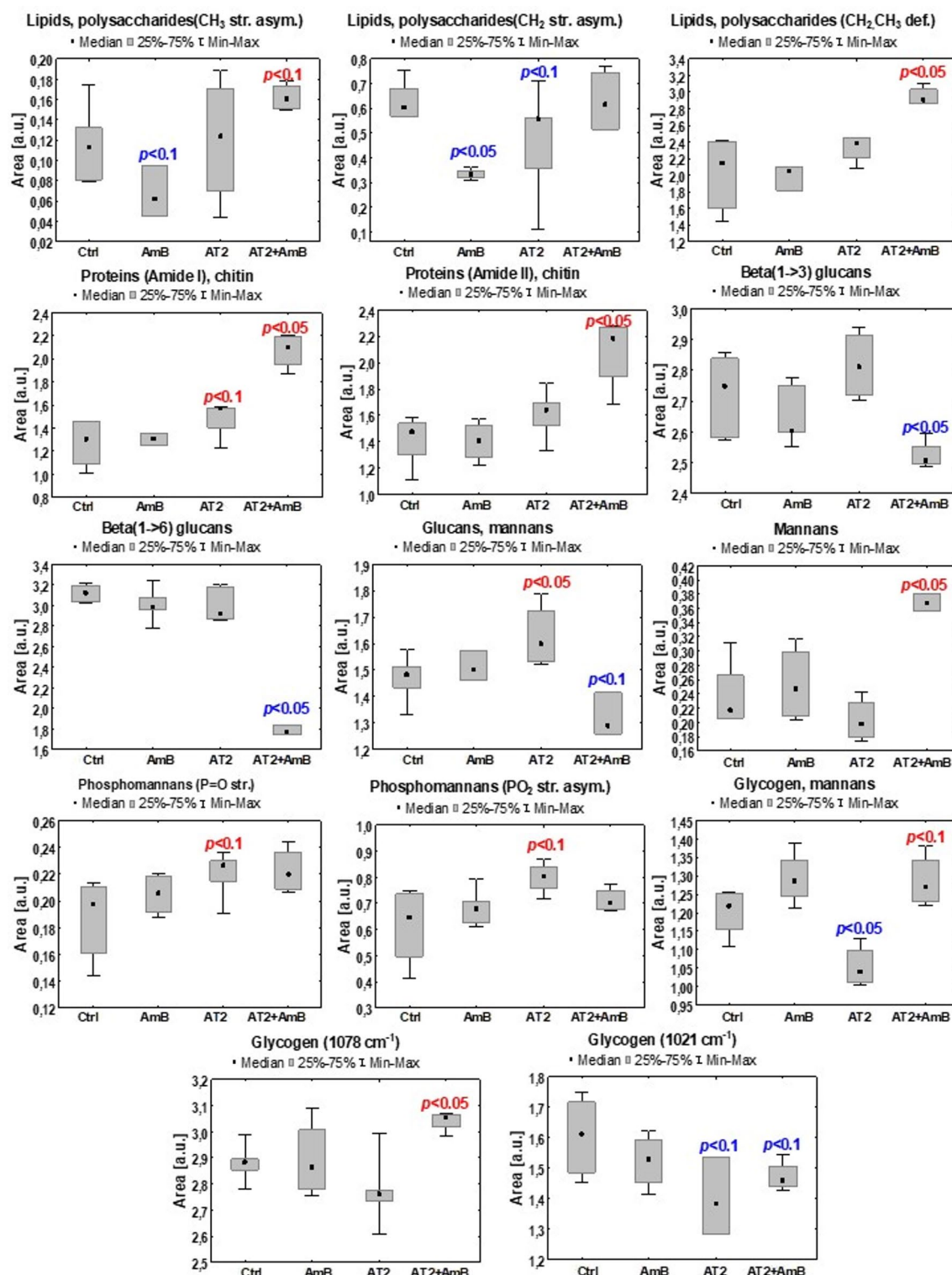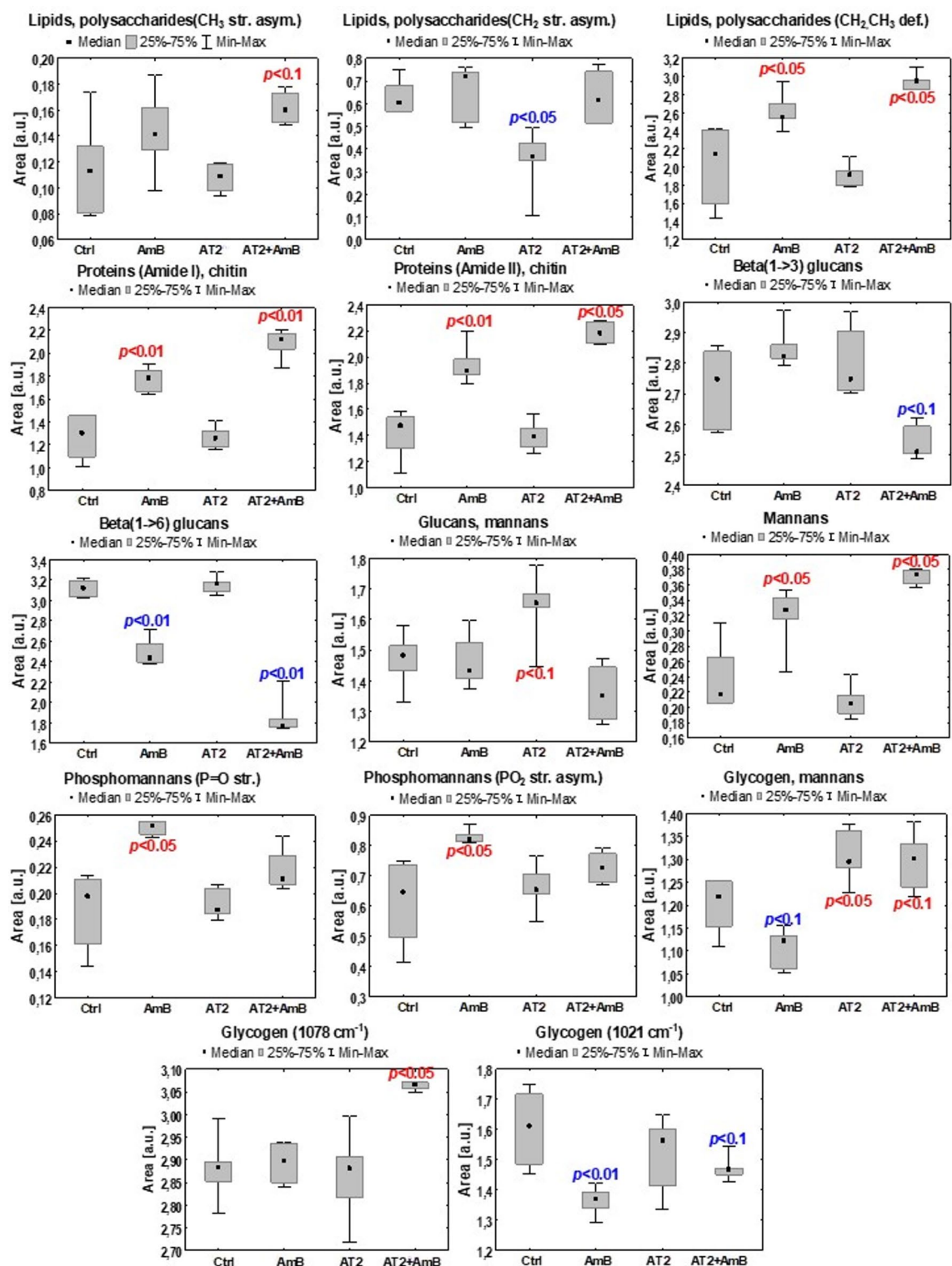
Fig. 7. Medians and minimum and maximum values of the intensity of selected absorption bands illustrating the differences between the groups: control, AmB, AT2, and AmB + AT2 for *C. albicans*. The graphs display the p-values from the Mann–Whitney U test for statistically significant changes, compared to the control (red color—increases, blue color—decreases).

Materials and methods
Strains
Fivereference strains were used in the experiment: *Candida albicans* NCPF 3153, *Candida krusei* ATCC 1424, *Candida glabrata* ATCC 15126, *Candida tropicalis* ATCC 13803 and *Candida parapsilosis* ATCC 22019. Prior
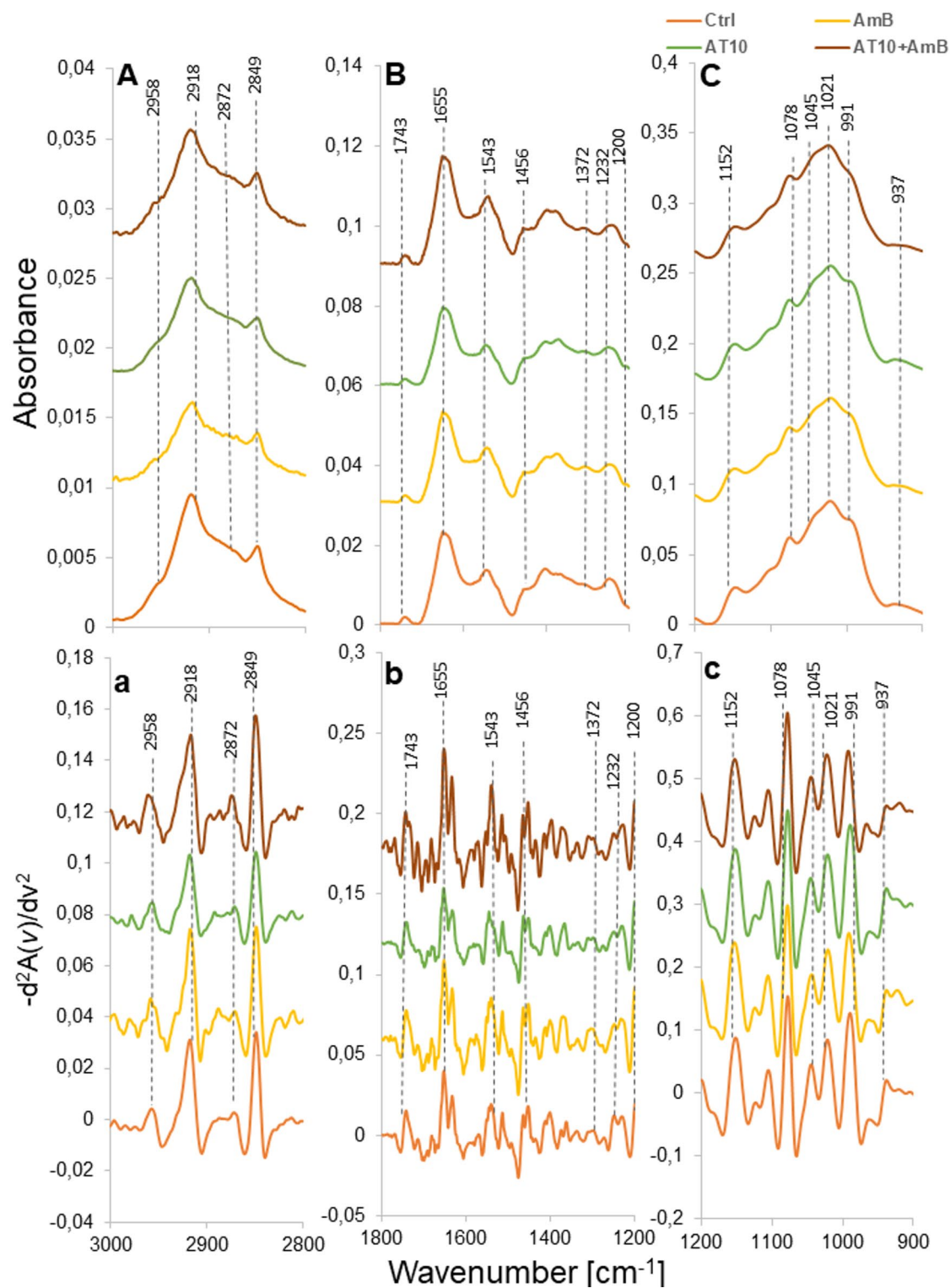
Fig. 8. Average IR spectra of *C. albicans* NCPF 3153 for the control, AmB (0.06 μg/mL), AT10 (32 μg/mL), and the combination of AT10 (32 μg/mL) and AmB (0.06 μg/mL) in the wavenumber ranges: (**A**) 3000–2800 cm^{-1}; (**B**) 1800–1200 cm^{-1}; (**C**) 1200–900 cm^{-1}; (**a**–**c**) negative second derivatives for spectra (**A**–**C**).

Fig. 9. Medians and minimum and maximum intensity values of selected absorption bands illustrating the differences between the groups: control, AmB, AT10, and AmB + AT10 for *C. albicans*. The graphs display the p-values from the Mann–Whitney U test for statistically significant changes, compared to the control (red color—increases, blue color—decreases).

Compound	Solvent Max Abs [nm]	Solvent Max FL [nm]	Stokes shift ([nm], [cm⁻¹])
AT1	DMSO/EtOH: 330	DMSO/EtOH: 385	DMSO/EtOH: 55 nm (4329 cm⁻¹)
AT2 *synergism with AmB)*	DMSO/EtOH: 325	DMSO/EtOH: 385	DMSO/EtOH: 60 nm (4795.2 cm⁻¹)
AT3	DMSO/EtOH: 330	DMSO/EtOH: 390	DMSO/EtOH: 60 nm (4662 cm⁻¹)
AT4	DMSO: 380	DMSO/EtOH: 450	DMSO: 70 nm; 4092 (78 cm⁻¹)
	EtOH: 350		EtOH: 100 nm; (6352.21 cm⁻¹)
AT5	DMSO: 370	DMSO: 590	DMSO: 220 nm; (10077.88 cm⁻¹)
	EtOH: 350	EtOH: 510	EtOH: 160 nm; (8963.59 cm⁻¹)
AT6	DMSO/EtOH: 310	DMSO/EtOH: 385	DMSO/EtOH: 75 nm (6284.03 cm⁻¹)
AT7	DMSO/EtOH: 310	DMSO/EtOH: 385	DMSO/EtOH: 75 nm (6284.03 cm⁻¹)
AT8	DMSO/EtOH: 320	DMSO/EtOH: 415	DMSO/EtOH: 70 nm (5608.97 cm⁻¹)
AT9	DMSO/EtOH: 285	DMSO/EtOH: 350	DMSO: 65 nm (6516.29 cm⁻¹)
			EtOH: 135 nm (11278.2 cm⁻¹)
AT10 *(synergism with AmB)*	DMSO/EtOH: 255	DMSO: 350 EtOH: 375	DMSO: 95 nm (10644.26 cm⁻¹)
			EtOH: 120 nm 12549.02 cm⁻¹)

Table 4. Location of the maxima of absorption and fluorescence emission bands in selected compounds in the two solvents used in the study.
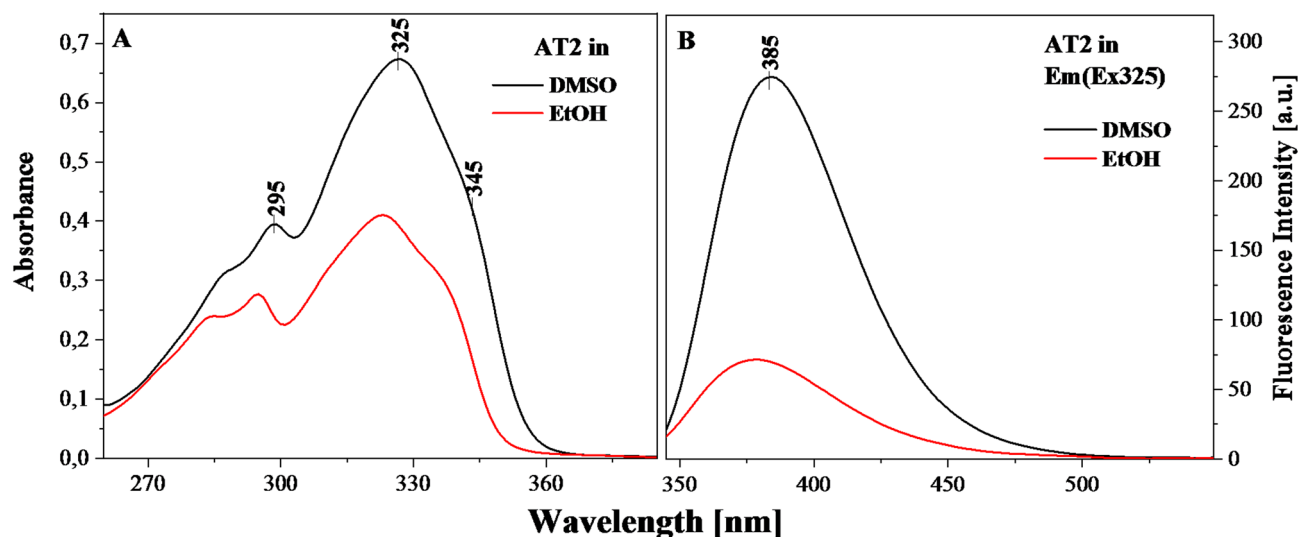
Fig. 10. Absorption and fluorescence emission spectra for AT2.

to each experiment, the fungi were pre-cultured in liquid YPD medium (1% yeast extract, 2% bactopepton, 2% glucose) in 0.01 mol/L phosphate buffer, pH 5.6, at 35 °C with shaking for 24 h.

Antifungal substances

Compound **1** was synthesized according to previously reported protocols[17,18]. Compounds **2** and **3** were synthesized in a similar manner except that 4-methyl-3-thiosemicarbazide was used for the synthesis of **2**, while salicylic acid was used for the synthesis of 3. Compounds **4–7** were synthesized via $FeCl_3$-mediated oxidative cyclization of corresponding thiosemicarbazones. Typically, an appropriate thiosemicarbazone and a 3-fold excess of $FeCl_3 \times 6H2O$ was refluxed in methanol for 6 h. The mixture was then cooled down and neutralized with the use of $Na_2S_2O_3$ (aq). The precipitate formed was filtered off, dried, and recrystallized from 50% ethanol (aq). In the case of compound **7**, the neutralized mixture was extracted with CH_2Cl_2. The organic layers were then combined and evaporated to dryness with the use of a rotary evaporator. The other thiadiazole derivatives **8–10** as well as amphotericin B (purity 80%) and fluconazole were purchased from Merck. The structures of the 1,3,4-thiadiazole derivatives tested are presented in Fig. 1. Samples of the synthesized thiadiazole derivatives are available from the authors upon request. Stock solutions of the test substances were obtained by dissolving 1 mg of powder in 100 µL of DMSO and diluted with medium to a concentration of 1 mg/mL.
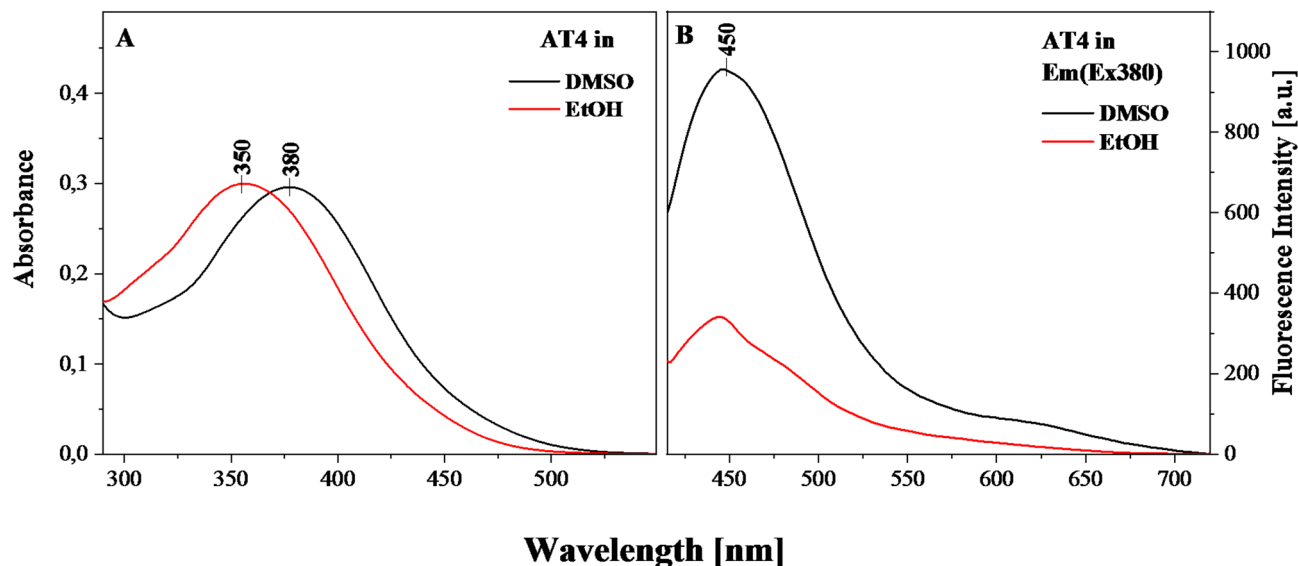
Fig. 11. Absorption and fluorescence emission spectra for AT4.

Antifungal activity

The antifungal activity of selected antibiotics and thiadiazoles was assessed by determining the minimum inhibitory concentrations (MIC) using the broth microdilution method, as previously described[12]. Standard methodological guidelines recommended by the European Committee on Antimicrobial Susceptibility Testing (EUCAST) were applied[19]. In brief, a fungal inoculum with a density of 0.5×10^5–2.5×10^5 cells/mL was prepared in RPMI 1640 culture medium (Sigma-Aldrich, R8755), buffered to pH 7.0 with 0.165 mol/L 3-(N-morpholino) propanesulfonic acid (MOPS), and supplemented with 2% glucose. The range of concentrations tested for the thiadiazoles was from 1 to 128 µg/mL. After inoculation, the plates were incubated for 48 h at 37 °C. Optical density was measured spectrophotometrically after 24 and 48 h of incubation using an EPOCH 2 microplate reader at a wavelength of 600 nm (OD_{600}). Complete inhibition of microbial growth after 48 h of incubation was designated as MIC_{100}. The results were compared to the control, which consisted of the medium with the yeast only. The MIC value was determined by calculating the percentage growth relative to the control in each replicate using the following formula: (OD_{600} of the treated sample)/(OD_{600} of the untreated sample) $\times$ 100.

Interactions between thiadiazoles and antibiotics

The interactions between thiadiazoles and antibiotics against *Candida* strains were investigated using the checkerboard microdilution technique, as previously described[10,12]. The thiadiazoles and antibiotics were serially diluted in RPMI in various combinations. The final concentrations ranged from 0.5 to 64 µg/mL for thiadiazoles, from 0.0125 to 2 µg/mL for amphotericin B (AmB), and from 0.5 to 64 µg/mL for fluconazole (Flu). *Candida* cells were added to each well at a final concentration of 0.5×10^5–2.5×10^5 cells/mL and incubated for 48 h at 37 °C. The MIC values were read visually after 48 h.

To assess the interactions between the thiadiazoles and the drugs, the fractional inhibitory concentration index (FICI) was used. The FIC index was calculated using the following formula: $\Sigma FIC = FIC\ A + FIC\ B$; where FIC A is the MIC of drug A in combination/MIC of drug A alone, and FIC B is the MIC of drug B in combination/MIC of drug B alone. The following criteria for interactions were adopted: $\Sigma FIC \leq 0.5$ = synergy; $\Sigma FIC > 0.5 - 1$ = additivity; $\Sigma FIC > 1$ to < 2 = indifference; $\Sigma FIC \geq 2$ = antagonism[20].

Selectivity index calculation

The calculations of the half-maximal inhibitory concentration (IC50; concentration of compounds resulting in 50% inhibition of cell viability) of the thiadiazoles tested (AT2 and AT10) were determined based on the results of the NR assay. The IC50 values were calculated by plotting a non-linear regression curve between the Log dose and the percentage (%) of cell viability using the GraphPad Prism 5 software. The selectivity index (SI) of the tested compounds was calculated using the following formula: SI = IC50 in µg/mL (normal NHDF cells)/MIC in µg/mL. SI value > 1.0 indicates a drug with efficacy against fungal cells greater than the toxicity against host cells.

Cytotoxic activity assessment (NR assay)

The cytotoxicity of thiadiazoles (AT2 and AT10) used alone or in combination with AmB against normal human dermal fibroblasts (NHDF, Lonza, CC-2511, Basel, Switzerland) and human renal proximal tubule epithelial cells (RPTECs, Lonza) was evaluated in an in vitro culture. The NHDF cells were cultivated in Dulbecco's modified Eagle medium nutrient mixture F-12 HAM (Sigma, D8062) supplemented with 10% fetal bovine serum (FBS), 100 U/mL penicillin, and 100 µg/mL streptomycin at 37 °C in a humid atmosphere containing 5% CO_2. The RPTECs were grown in epithelial basal medium (REBM) supplemented with a growth factor cocktail (Lonza catalog no. CC-3190) and gentamycin 100 µg/mL (Sigma-Aldrich Chemical Co. (St. Louis, MO, USA). The
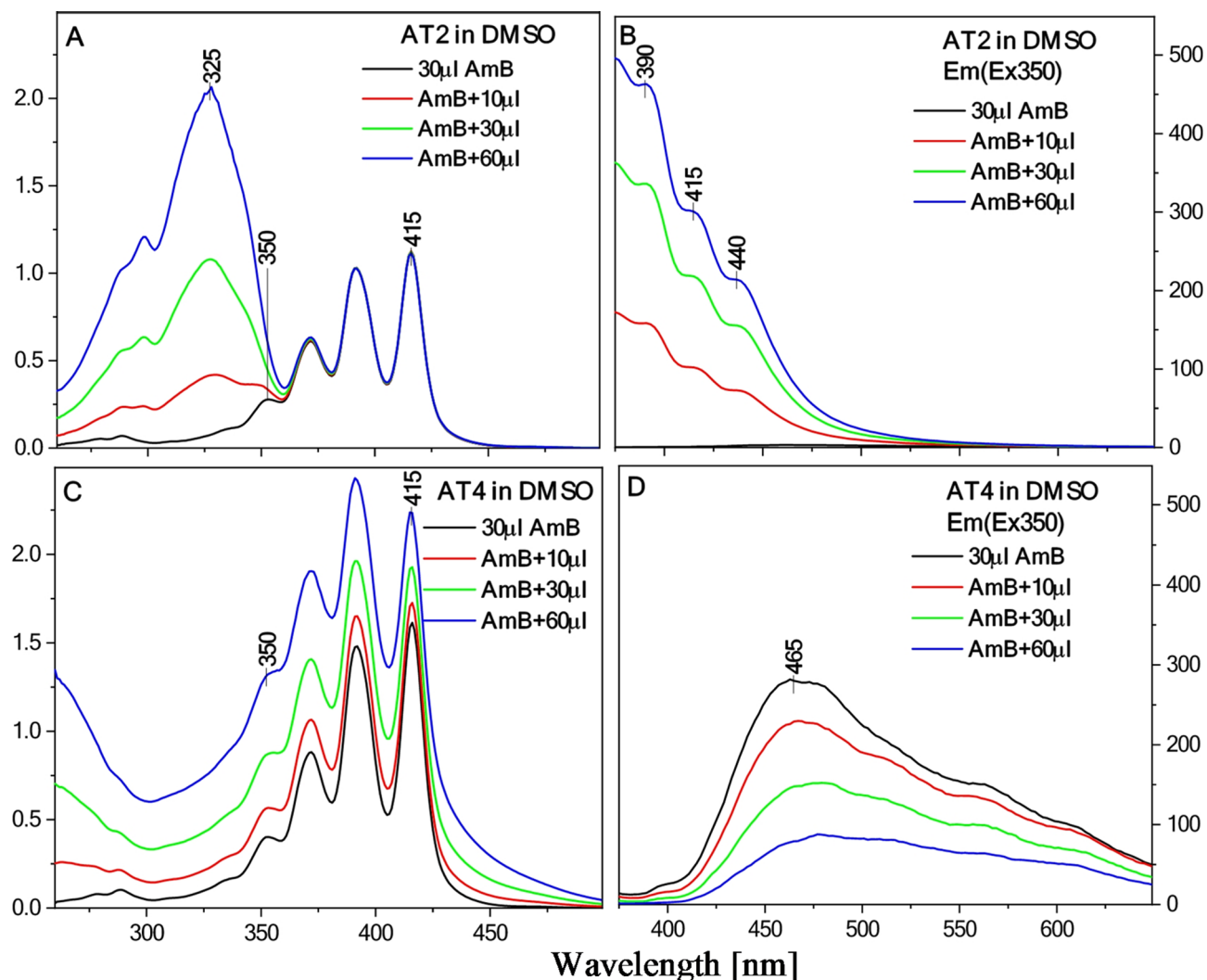
Fig. 12. (**A**, **C**) Absorption spectra for selected systems capable of synergism (**A**) and incapable of synergism (**C**). (**B**, **D**) Examples of fluorescence emission spectra corresponding to the electronic absorption spectra for the selected compounds.

viability of treated and control cells was assessed by the Neutral Red (NR) assay (Sigma-Aldrich, St Louis, MO, USA). The procedure was performed as described previously [Czerwonka et al. 2018]. Briefly, the NHDF cells were seeded into 96-well microplates at a high density of 4×10^4 cells/well and treated with various concentrations (4–256 µg/mL) of AT2 or AT10 prepared in 2% medium. In some experiments, the cells were exposed to single doses of AmB and thiadiazoles (AT2 or AT10 at 32 and 64 µg/mL) and combined with amphotericin (1.25 µg/mL or 0.25 µg/mL). The controls were left untreated. Similarly, the RPTEC cells were cultured in 96-well plates in appropriate growth medium and cultured in the presence of various concentrations of AT10 and AmB and combinations of these compounds. After 48-hour exposure, the medium was poured out and the cells of each well received 100 µL of a new medium containing 40 µg/mL NR dye. Following 3 h of incubation at 37 °C, the cells were washed with phosphate buffer saline (PBS, 2x), fixed with formaldehyde–CaCl2 solution, and extracted with an acetic acid- ethanol solution. Subsequently, the plates were transferred to a shaker and left for 30 min at room temperature. After this time, the lysosomal activity was determined spectrophotometrically at 540 nm using a microplate reader (Molecular Devices Corp., Emax, Menlo Park, CA). The amount of dye released from acidic organelles was proportional to the number of viable cells. The results of viability, presented as arithmetic mean ± SD, were analyzed using GraphPad Prism (GraphPAD Software Inc. version 5, San Diego, CA, USA). Statistical significance was calculated with one-way ANOVA test, followed by Dunnett's or Tukey's multiple comparison tests. p values < 0.05 were considered significant.

ATR-FTIR spectroscopy

To investigate the molecular mechanisms underlying the synergistic effects of thiadiazoles (AT2 and AT10) in combination with amphotericin B (AmB) against *C. albicans*, attenuated total reflectance Fourier-transform infrared spectroscopy (ATR-FTIR) was employed. *C. albicans* cells were incubated for 48 h with AT2 (32 µg/
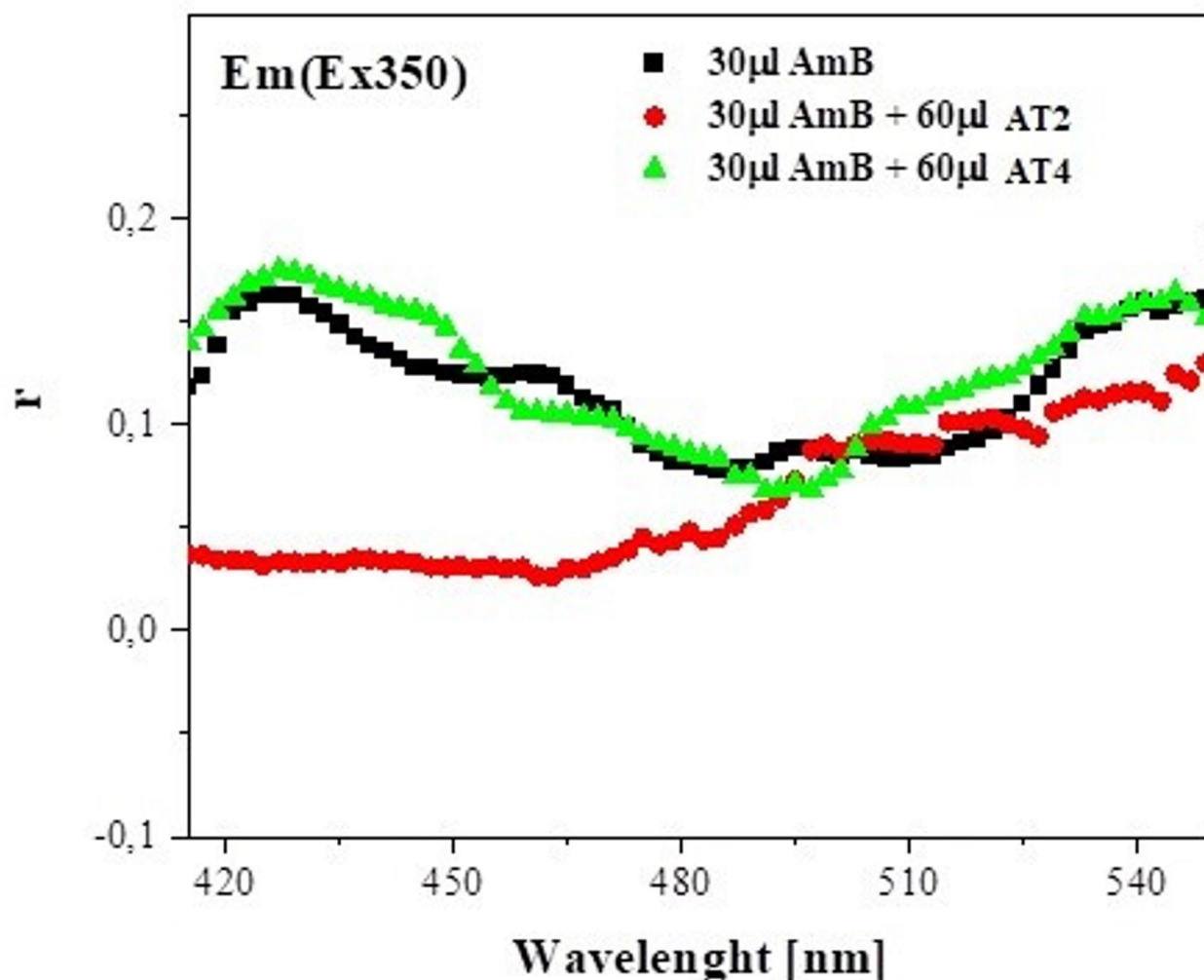
Fig. 13. Results of fluorescence anisotropy measurements for the selected compounds (AT2 and AT4) and AmB.

mL), AmB (0.06 µg/mL), and their mixture and with AT10 (32 µg/mL), AmB (0.03 µg/mL), and their mixture. The control cells of *C. albicans* were incubated for 48 h without treatment. The fixation and sample preparation procedure was described previously[12]. Fixed cells were placed on a ZnSe crystal and air-dried. ATR-FTIR spectra for all analyzed isolates were recorded in the wavelength range of 4000–700 cm⁻¹ using the FTIR spectrometer VERTEX 70 (Bruker Optic GmbH, Germany) with an MCT detector. IR spectra were acquired with a spectral resolution of 2 cm⁻¹, averaging 64 scans for each sample and background spectrum. Baseline correction, vector normalization, calculation of inverted second derivatives of the spectra, and determination of the areas of the investigated absorption bands were performed using OPUS 7.5 software (Bruker Optic GmbH, Ettlingen, Germany). Graphical processing of the IR spectra and their second derivatives was carried out using Microsoft Excel. Statistical analysis of the changes in the IR spectra of *C. albicans* treated with AT2, AT10, and AmB as well as AT2 + AmB and AT10 + AmB, compared to the control, was performed using STATISTICA 7.1 software (StatSoft, Inc., Tulsa, OK, USA, 2005). The non-parametric Mann-Whitney U test was used to demonstrate statistically significant differences.

Electronic absorption spectroscopy (UV–Vis) and fluorescence spectroscopy

Electronic absorption spectra of were recorded using a double-beam UV-vis spectrophotometer Cary 300 Bio (Varian) equipped with a thermostatted tray holder with a 6×6 multi-cell Peltier block. Temperature was controlled with a thermocouple probe (Cary Series II from Varian) placed directly in the sample.

A Cary Eclipse spectrofluorometer (Varian) was employed for measurements of fluorescence excitation, emission, and synchronous spectra, all performed at 22 °C. The fluorescence spectra were recorded with 0.5 nm resolution applying the lamp and photomultiplier spectral characteristic corrections. Grams/AI 8.0 software (Thermo Electron Corporation; Waltham, Massachusetts, United States) was used in the analysis of the recorded data.

Anisotropy

Steady-state fluorescence anisotropy r was calculated from the polarized components of fluorescence emission according to the equation:

$$r = \frac{I_{VV} - GI_{VH}}{I_{VV} + 2GI_{VH}}$$

where: I_{VH} is the intensity of the vertically excited, horizontally observed emission, I_{VV} is the intensity of the vertically excited, vertically observed emission, and G is the geometrical factor which corrects for the system's polarization bias. A wire grid polarizer was used on the excitation to allow UV light transmission.

Discussion

In recent years, the development of antifungal drugs has become an area of intensive research due to the increasing threat posed by fungi resistant to existing medications[21–23]. The study of the antifungal activity of selected substances revealed significant differences in their efficacy against *Candida* strains. Typical strains *C. albicans* NCPF 3153, *Candida krusei* ATCC 1424, *Candida glabrata* ATCC 15126, *Candida tropicalis* ATCC 13803 and *C. parapsilosis* ATCC 22019 with different susceptibilities to AmB were selected to ensure reproducibility of the results. Among the 10 compounds tested, AT2 exhibited the highest activity, as confirmed by the minimum inhibitory concentration (MIC$_{100}$) values of 128 μg/mL after 48 h of incubation of both reference strains. Additionally, at a concentration of 16 μg/mL, AT2 inhibited fungal growth by about 40%, indicating its potential in reducing the population of *Candida* at lower doses. Although it exhibited strong growth inhibition (90–100%) after 24 h of incubation at the highest tested concentration, substance AT1 was not as effective over a longer period, suggesting the possibility of fungal adaptation or rapid metabolism of the substance. Conversely, despite its weaker antifungal activity, compared to AT2 and AT1, AT6 may still be a valuable compound, especially in the context of lower doses. In terms of interactions between thiadiazoles and antibiotics, only two compounds (AT2 and AT10) demonstrated synergistic activity with amphotericin B (AmB) against selected *Candida* species after 24 h and 48 h of incubation. We assessed the interaction results at both 24 and 48 h to capture potential time-dependent effects of the combined compounds. The 24-hour time point allowed us to evaluate early interactions and immediate antifungal effects, while the 48-hour assessment provided insights into prolonged exposure and possible delayed synergistic or antagonistic effects. Notably, the synergistic effect persisted after 48 h, indicating sustained antifungal activity of the combined treatment over time. The obtained results align with our previous studies, which also showed synergistic antifungal interactions of amphotericin B (AmB) with selected 1,3,4-thiadiazole derivatives, such as C1 and NTBD[10–12]. These derivatives demonstrated strong synergistic activity with AmB against various *Candida* species, including those with reduced sensitivity to AmB and azole-resistant isolates. Interestingly, none of the examined substances showed significant interaction with fluconazole. While azoles target ergosterol biosynthesis, thiadiazole derivatives may act on different components of the fungal cell wall, which may potentially explain the lack of synergy with fluconazole. This observation further emphasizes the specificity of the synergistic effect between thiadiazoles and AmB. The absence of antagonistic interactions also suggests that these compounds do not inhibit the antifungal efficacy of AmB, further supporting their potential use in combination therapies. In further studies, we will use our results and the developed methodology to investigate the synergy of AT2 and AT10 with amphotericin B against clinical (wild-type) strains of various species isolated from different infections.

Our in vitro cytotoxic studies on normal human cells may provide significant information regarding the safety of these compounds in biological applications. The results of the NR assay performed on human dermal fibroblasts (NHDF cell line) showed that AT2 and AT10 (with potential antifungal activity) disrupted the integrity of cell membrane and killed these cells only at high doses (the calculated IC50 values for AT2 and AT10 were 130.5 μg/mL and 477.2 μg/mL respectively). Moreover, when used in non-toxic doses together with AmB, they showed the ability to increase the survival of the NHDF cell culture. The protective effect of these compounds on AmB-treated fibroblasts may make them applicable as a therapeutic agent in the treatment of surface mycoses.

Also in relation to the human renal proximal tubule epithelial cells (RPTECs), AT10 exhibited minimal toxicity over a wide range of concentrations (from 0.50 to 64.00 μg/mL), confirming its potential safety in therapy, particularly in comparison to other compounds with strong antimicrobial activity that often cause a negative cytotoxic impact on host cells. The additional studies on the effect of AT10 administered with AmB demonstrated no cytotoxic effects against renal cells, which is extremely important regarding the potential use of AT10 in combined therapy. This may indicate the possibility of using AT10 as a potential adjuvant that alleviates the toxic effects of amphotericin B on host cells. It is also worth noting that the presence of AT10 did not negatively affect the efficacy of amphotericin B itself, which is an important factor in assessing potential combination therapies. In the literature, amphotericin B is known for its high effectiveness against various fungal pathogens, but its toxicity, particularly to renal tubule cells, is a serious clinical limitation. Therefore, the potential for AT10 and AT2 to reduce the cytotoxicity of amphotericin B without affecting its therapeutic action could open new perspectives for safer and more effective antifungal therapies.

The results of the ATR-FTIR analysis confirm significant biochemical changes in *C. albicans* cells subjected to the action of the 1,3,4-thiadiazole derivatives (AT2 and AT10), amphotericin B (AmB), and their combinations. Compared to the control group, differences were observed in the intensity of bands corresponding to the main components of the cell wall, particularly glucans and mannans. These results suggest that the action of the studied compounds may affect the integrity of the cell wall in *C. albicans* by disrupting the structure of β-glucans, which are crucial for its stability[24–26]. The statistically significant decrease in the intensity of bands associated with β(1→3) and β(1→6) glucans (at 1152 cm⁻¹ and 991 cm⁻¹, respectively) in the combinations AT2 + AmB

and AT10 + AmB, compared to the control, indicates weakening of the cell wall structure, which may have contributed to the increased sensitivity of the fungal cells to the action of the antibiotics[12,27,28]. Moreover, the increase in the intensity of bands corresponding to mannans (at 961 cm⁻¹) may suggest increased biosynthesis of these polysaccharides as a result of cellular stress induced by the studied substances[29,30]. Additionally, correlations between the content of mannans and amide I and II proteins were observed both for AmB alone and for the combinations, with more pronounced increases in the mixtures, suggesting a synergistic effect. This correlation may be linked to changes in the mannoprotein content, which determine the porosity of the outer cell membrane, potentially leading to its weakening and increasing cell susceptibility to antibiotics[29,31].

Given the results related to UV-Vis and fluorescence spectroscopy as well as fluorescence anisotropy measurements, it should be underlined that they indicated a strong impact of aggregation effects on the analyzed systems. Most importantly, aggregation significantly affects the mechanisms related to the synergistic interaction between AmB molecules and certain thiadiazoles. As clearly presented in Figs. 12 and 13, in the case of the AT2 compound, both the emission spectra and fluorescence anisotropy measurements clearly indicated effects related to monomerization of AmB molecules. We observed a clear increase in emission and decrease in fluorescence anisotropy, both of which suggest elevated levels of AmB monomerization. Notably, the biological tests confirmed the promising synergism between the two molecules in question. On the other hand, in the case of AT4, i.e. a molecule that showed no capacity for synergism with AmB, the results were exactly the opposite, indicating increased absorption within the analyzed spectral region, an effect thoroughly described in literature and associated with aggregation of AmB molecules. The fluorescence emission spectra measured for this compound revealed a decrease in the intensity of fluorescence emission, i.e. increased aggregation of the analyzed molecules, including AmB molecules. Furthermore, the relatively high level of anisotropy, comparable to that observed for AmB alone, also corroborated the hypothesis formulated in this study. It can be concluded that a key aspect in explaining the synergistic properties of compositions containing certain molecules from the group of 1,3,4-thiadiazoles and amphotericin B relates to the impact of particular molecules on the aggregation/disaggregation of AmB. At the same time, as follows from literature, the toxicity of AmB is often associated with the effects of molecular aggregation. Other reports indicate that even partial monomerization of AmB can significantly improve its therapeutic effectiveness. It seems, therefore, that the 1,3,4-thiadiazoles triggering a desirable therapeutic effect in combinations with AmB must interact with the antibiotic in places where AmB molecules normally interact with each other to form aggregates.

In our future research into these effects, we intend to analyze these processes in even greater detail by employing a range of molecular spectroscopy methods.

Conclusions

Among the analyzed 1,3,4-thiadiazole derivatives, AT2 exhibits the highest potential for enhancing the sensitivity of *Candida* cells to amphotericin B (AmB). AT2 shows superior synergistic interactions with AmB against selected *Candida* species, particularly *C. albicans*, *C.glabrata* and *C. parapsilosis*. Additionally, both AT2 and AT10 demonstrate minimal cytotoxicity towards normal human dermal fibroblasts and renal proximal tubule epithelial cells, indicating their safety for potential therapeutic applications. The mechanism underlying the observed synergy appears to involve the disruption of cell wall integrity, as evidenced by changes in the biochemical composition of *C. albicans*, specifically affecting β-glucans and mannan biosynthesis.

The analyses performed with the use of absorption spectroscopy and electronic fluorescence spectroscopy as well as fluorescence anisotropy measurements indicated that that the AT2 and AT10 molecules are most likely capable of triggering disaggregation of AmB aggregates, which reduces the toxicity of the antibiotic, while also improving its therapeutic effects related to the antimycotic properties of these molecules. The strongest evidence supporting this observation follows from the results of fluorescence emission measurements of AT2 and AT4 and from the measurements of fluorescence anisotropy conducted for the selected systems.

Moreover, AT2 and AT10 do not impair the antifungal efficacy of AmB, making them promising candidates for combination therapy. However, to translate these findings into clinical practice, further studies assessing the in vivo efficacy and safety of these combinations are essential. Overall, this research highlights the potential of thiadiazole derivatives as valuable adjuncts in antifungal therapy, providing new avenues for combating resistant fungal infections.

Data availability
The data can be available upon request from the corresponding author.

References
1. Barantsevich, N. & Barantsevich, E. Diagnosis and treatment of invasive candidiasis. *Antibiotics* **11**, 718 (2022).
2. McCarty, T. P., White, C. M. & Pappas, P. G. Candidemia and invasive candidiasis. *Infect. Dis. Clin. N. Am.* **35**, 389–413 (2021).
3. Zhang, Z., Zhu, R., Luan, Z. & Ma, X. Risk of invasive candidiasis with prolonged duration of ICU stay: a systematic review and meta-analysis. *BMJ Open.* **10**, e036452 (2020).
4. McKeny, P. T., Nessel, T. A. & Zito, P. M. *Antifungal Antibiotics* (StatPearls Publishing, 2022).
5. Pianalto, K. M. & Alspaugh, J. A. New horizons in antifungal therapy. *J. Fungi.* **2**, 26 (2016).
6. Wall, G., Lopez-Ribot, J. L., Current & Antimycotics New prospects, and future approaches to antifungal therapy. *Antibiotics* **9**, 445 (2020).
7. Lee, Y., Puumala, E., Robbins, N. & Cowen, L. E. Antifungal drug resistance: molecular mechanisms in Candida albicans and beyond. *Chem. Rev.* **121**, 3390–3411 (2021).
8. Lockhart, S. R. Candida auris and multidrug resistance: defining the new normal. *Fungal Genet. Biol.* **131**, 103243 (2019).

9. Odds, F. C. Synergy, antagonism, and what the chequerboard puts between them. *J. Antimicrob. Chemother.* **52**, 1–1 (2003).
10. Chudzik, B. et al. Synergistic antifungal interactions of amphotericin B with 4-(5-methyl-1,3,4-thiadiazole-2-yl) benzene-1,3-diol. *Sci. Rep.* **9**, 12945 (2019).
11. Chudzik, B. et al. Antifungal effects of a 1,3,4-thiadiazole derivative determined by cytochemical and vibrational spectroscopic studies. *PLOS ONE.* **14**, e0222775 (2019).
12. Dróżdż, A. et al. Synergistic antifungal interactions between antibiotic amphotericin B and selected 1,3,4-thiadiazole derivatives, determined by Microbiological, cytochemical, and molecular spectroscopic studies. *Int. J. Mol. Sci.* **24**, 3430 (2023).
13. Dróżdż, A. et al. Effect of antibiotic amphotericin B combinations with selected 1,3,4-Thiadiazole derivatives on RPTECs in an in vitro model. *Int. J. Mol. Sci.* **23**, 15260 (2022).
14. Movasaghi, Z. & Rehman, S. Ur Rehman, D.I. Fourier transform infrared (FTIR) spectroscopy of biological tissues. *Appl. Spectrosc. Rev.* **43**, 134–179 (2008).
15. Budziak-Wieczorek, I. et al. Spectroscopic characterization and assessment of Microbiological potential of 1,3,4-thiadiazole derivative showing ESIPT dual fluorescence enhanced by aggregation effects. *Sci. Rep.* **12**, 22140 (2022).
16. David, M., Budziak-Wieczorek, I., Karcz, D., Florescu, M. & Matwijczuk, A. Insight into dual fluorescence effects induced by molecular aggregation occurring in membrane model systems containing 1,3,4-thiadiazole derivatives. *Eur. Biophys. Journal: EBJ.* **50**, 1083–1101 (2021).
17. Karcz, D. et al. Structural features of 1,3,4-Thiadiazole-Derived ligands and their Zn(II) and Cu(II) complexes which demonstrate synergistic antibacterial effects with Kanamycin. *Int. J. Mol. Sci.* **21**, 5735 (2020).
18. Karcz, D.et al. Design, Spectroscopy, and Assessment of Cholinesterase Inhibition and Antimicrobial Activities of Novel Coumarin–Thiadiazole Hybrids. International Journal of Molecular Sciences23, 6314 (2022).
19. ESCMID European Committee for Antimicrobial Susceptibility Testing (EUCAST). Method for the determination of broth Dilution minimum inhibitory concentrations of antifungal agents for yeasts. *EUCAST E Def.* **7**, 4 (2023).
20. Novy, P., Rondevaldova, J., Kourimska, L. & Kokoska, L. Synergistic interactions of Epigallocatechin gallate and Oxytetracycline against various drug resistant Staphylococcus aureus strains in vitro. *Phytomedicine* **20**, 432–435 (2013).
21. Logan, A., Wolfe, A. & Williamson, J. C. Antifungal resistance and the role of new therapeutic agents. *Curr. Infect. Dis. Rep.* **24**, 105–116 (2022).
22. Hoenigl, M. et al. Novel antifungals and treatment approaches to tackle resistance and improve outcomes of invasive fungal disease. *Clin. Microbiol. Rev.* **37**, e0007423 (2024).
23. Mota Fernandes, C. et al. The future of antifungal drug therapy: novel compounds and targets. *Antimicrob. Agents Chemother.* **65** (2021).
24. Garcia-Rubio, R., de Oliveira, H. C. & Rivera, J. & Trevijano-Contador, N. The fungal cell wall: Candida, Cryptococcus, and Aspergillus species. *Front. Microbiol.* **10** (2020).
25. François, J. & Parrou, J. L. Reserve carbohydrates metabolism in the yeast Saccharomyces cerevisiae. *FEMS Microbiol. Rev.* **25**, 125–145 (2001).
26. Aimanianda, V. et al. Cell wall β-(1,6)-Glucan of Saccharomyces cerevisiae: STRUCTURAL CHARACTERIZATION AND IN SITU SYNTHESIS*. *J. Biol. Chem.* **284**, 13401–13412 (2009).
27. Lowman, D. W. et al. Glucan and glycogen exist as a covalently linked macromolecular complex in the cell wall of Candida albicans and other Candida species. *Cell. Surf.* **7**, 100061 (2021).
28. Arvindekar, A. U. & Patil, N. B. Glycogen—a covalently linked component of the cell wall in Saccharomyces cerevisiae. *Yeast* **19**, 131–139 (2002).
29. De Nobel, J. G., Klis, F. M., Priem, J., Munnik, T. & Van Den Ende, H. The glucanase-soluble mannoproteins limit cell wall porosity in Saccharomyces cerevisiae. *Yeast* **6**, 491–499 (1990).
30. González-Hernández, R. J. et al. Phosphomannosylation and the functional analysis of the extended Candida albicans MNN4-Like gene family. *Front. Microbiol.* **8** (2017).
31. Harris, M., Mora-Montes, H. M., Gow, N. A. R. & Coote, P. J. Loss of mannosylphosphate from Candida albicans cell wall proteins results in enhanced resistance to the inhibitory effect of a cationic antimicrobial peptide via reduced peptide binding to the cell surface. *Microbiology* **155**, 1058–1070 (2009).

Author contributions

D.K.: conceptualisation, investigation, formal analysis, methodology, validation, writing – original draft preparation; Adrianna Sławińska-Brych: investigation, methodology, resources, writing – reviewing and editing; A.D.:investigation, methodology, resources, writing – reviewing and editing; A.O.: conceptualisation, resources, supervision, project administration, writing – reviewing and editing; A.B.: investigation, methodology, resources, writing – reviewing and editing; A.M.: investigation, methodology, resources, writing – reviewing and editing, D.K.: investigation, methodology, resources, writing – reviewing and editing, M.K.D: methodology, validation, writing – reviewing and editing; J.M.G.: methodology, validation, writing – reviewing and editing; C.K.R: methodology, validation, writing – reviewing and editing; J.A.: methodology, validation, writing – reviewing and editing; M.S. :methodology, validation, writing – reviewing and editing; W.D.: conceptualisation, resources, supervision, project administration, writing – reviewing and editing; A.S.: conceptualisation, resources, supervision, project administration, writing – reviewing and editing; M.G: conceptualisation, resources, supervision, founding acquisition, project administration, writing –reviewing and editing.

Funding

Declarations

Competing interests

The authors declare no competing interests.

Consent to participate

All Authors agree to participate in the published version of the manuscript.

Additional information

Correspondence and requests for materials should be addressed to D.K. or M.G.

Reprints and permissions information is available at www.nature.com/reprints.

Publisher's note Springer Nature remains neutral with regard to jurisdictional claims in published maps and institutional affiliations.